

JET PRODUCTION AND HIGH p_T PHENOMENA IN PHOTON-PHOTON REACTIONS*

NORBERT WERMES[†]

Stanford Linear Accelerator Center

Stanford University, Stanford, California 94305

ABSTRACT

The status of experimental investigations of high p_T phenomena and jet production in photon-photon collisions is reviewed. Taking the challenging questions on hard scattering processes in $\gamma\gamma$ reactions as a guide, the experimental approach to these questions is summarized. Results from the PETRA experiments CELLO, JADE, PLUTO, and TASSO are presented including preliminary results on the Q^2 -dependence of jet cross sections. Experimental limitations and background problems are discussed.

Zusammenfassung – Es wird ein Überblick über den Stand experimenteller Untersuchungen von high- p_T Phänomenen und der Erzeugung von Jets in Photon-Photon Wechselwirkungen gegeben. Anhand der herausfordernden Fragen bezüglich harter Streuprozesse in $\gamma\gamma$ Reaktionen wird der experimentelle Ansatz zur Beantwortung dieser Fragen zusammengefasst. Ergebnisse der PETRA Experimente CELLO, JADE, PLUTO und TASSO werden präsentiert. Vorläufige Untersuchungen der Q^2 -Abhängigkeit von Jet-Wirkungsquerschnitten sowie experimentelle Einschränkungen und Untergrundprobleme werden diskutiert.

* Work supported by the Department of Energy, contract DE-AC03-76SF00515.

[†] Alexander von Humboldt Fellow.

1. INTRODUCTION

This talk reviews experimental results on hard scattering reactions in $\gamma\gamma$ collisions via high p_T phenomena.

The talk is divided into three parts. First I shall try to list the physics challenges for photon-photon experiments, in the context of hard scattering processes at high p_T . In the main part the experimental approach to these challenging questions is discussed. It will be explained why we believe that hard scattering processes do exist. Then the explicit jet-searches performed by the different experiments are reviewed. Finally I shall conclude with an attempt to assess to what extent the challenging questions can be answered.

Many theoreticians¹ believe that photon-photon collisions and particularly the high p_T hard scattering phenomena are perhaps the cleanest laboratory for testing QCD. The arguments are that there are only fundamental particles involved and the processes are computable in QCD. Also, when approaching $\gamma\gamma$ scattering through $e^+e^- \rightarrow e^+e^- + \text{hadrons}$ in e^+e^- storage rings the corresponding structure functions in the "hard scattering expansion" are relatively simple compared to hadron-hadron interactions. There are no spectator jets accompanying the leading order $\gamma\gamma \rightarrow q\bar{q}$ reaction as in pp scattering which makes the experimental situation much cleaner. Last, but not least, the photon itself is a very direct probe of matter and the fact that the photon's Q^2 can be varied in e^+e^- collisions is very useful to disentangle hadronic and pointlike reactions in $\gamma\gamma$ collisions.

In the following I want to list a not necessarily complete set of explicit tasks being formulated by theory and challenging the experiments.

- $\gamma\gamma \rightarrow q\bar{q}$ scattering at high transverse momenta allows one to test the quark propagator at large p^2 . This should be much cleaner in $\gamma\gamma$ collisions than in e^+e^- reactions via $e^+e^- \rightarrow q\bar{q}g$ because no uncertainties introduced through the strong coupling constant α_s confuse the issue. In the same context there is a question whether current or constituent quark masses appear in the quark propagator.
- In their epochal paper² in 1971 Berman, Bjorken and Kogut pointed out that for pointlike hard scattering processes like $\gamma\gamma \rightarrow q+X$ the jet (quark)-trigger cross sections should scale as

$$E \frac{d\sigma}{d^3p} (\gamma\gamma \rightarrow \text{jet} + X) \propto \frac{1}{p_T^4} f(x_T, \theta_{c.m.}) \quad , \quad (1)$$

where $x_T = 2p_T/\sqrt{s}$, $\theta_{c.m.}$ = center-of-mass angle of jet, p_T = transverse jet-momentum with respect to the $\gamma\gamma$ axis. This typical scaling behaviour should be tested in $\gamma\gamma \rightarrow \text{jet} + X$ cross sections and in inclusive particle cross sections at high p_T .

- $\gamma\gamma \rightarrow q\bar{q}$ scattering provides a useful tool to test the quark charges and resolve the question of fractionally or integrally charged quarks. Let me spend a few words on why $\gamma\gamma$ scattering is unique for this. Quark charges in models which satisfy the modified Gell-Mann-Nishijima

relation

$$Q = \left(T_3 + \frac{Y}{2}\right) + \frac{1}{3} t \quad (2)$$

where T_3 and $Y/2$ are flavour generators and t is an arbitrary number which may depend on colour, can be assigned in a very general way³

	<i>u</i>	<i>d</i>	<i>s</i>	<i>c</i>	
<i>R</i>	z_R	$z_R - 1$	$z_R - 1$	z_R	
<i>B</i>	z_B	$z_B - 1$	$z_B - 1$	z_B	
<i>Y</i>	z_Y	$z_Y - 1$	$z_Y - 1$	z_Y	

(3)

where R,B,Y denote different colours and the constraint that $z_R + z_B + z_Y = 2$, which follows from the fact that the $\Delta^{++}(u_R, u_B, u_Y)$ has charge +2, has to be obeyed. In the fractionally charged quark model (FCQ), also called Gell-Mann-Zweig model,⁴ one has $z_R = z_B = z_Y = 2/3$; in integrally charged quark models (ICQ) originally invented by Han and Nambu⁵ the assignment is $z_R = 0$, $z_B = z_Y = 1$. In this nomenclature the photon can be considered as

$${}^{\prime}\gamma^{\prime} \sim (e_f q \bar{q}, R\bar{R} + B\bar{B} + Y\bar{Y}) + \left(\left(z_R - \frac{2}{3}\right) q \bar{q}, R\bar{R} - Y\bar{Y}\right) + \left(\left(z_B - \frac{2}{3}\right) q \bar{q}, B\bar{B} - Y\bar{Y}\right) \quad (4)$$

where e_f = flavour-charge of quarks (2/3, -1/3). The notation $(q \bar{q}, R\bar{R} + B\bar{B} + Y\bar{Y})$ means $(q_R \bar{q}_R + q_B \bar{q}_B + q_Y \bar{q}_Y)$ and it is easy to see that in (4) the photon is decomposed into a flavour and a colour part. Expressing (4) in terms of flavour and colour multiplets we find in the particular case of the ICQ-model

$${}^{\prime}\gamma^{\prime} \sim (\{NS\}_F, \{1\}_C) - (\{1\}_F, \{8\}_C) \quad (5)$$

where F,C denote flavour and colour and *NS* represents 'non-singlet' ($\{NS\}_F = \{8\}_F$ in case of $SU(3)_F$). Note that for FCQ models $z_\alpha - (2/3) = 0$ for $\alpha = R, B$ and therefore there is no colour octet piece of the photon in these models. The colour octet part of the photon is responsible for a different value of $R_{\gamma\gamma}$ in the two quark model alternatives. While in one photon annihilation (Fig. 1) the final state colour singlet can only be generated by a colour singlet photon, in two photon reactions (Fig. 2) two colour octet photons can produce a colour singlet final state ($\{8\} \otimes \{8\} = \{1\} \oplus \{8\} \oplus \{8\} \oplus \{10\} \oplus \{1\bar{0}\} \oplus \{27\}$). Thus⁶

$$R_{\gamma\gamma} = \frac{d\sigma/dt(\gamma\gamma \rightarrow q\bar{q})}{d\sigma/dt(\gamma\gamma \rightarrow \mu\mu)} = \left\{ \frac{3 \cdot \sum_i e_i^4}{1/3 \cdot \sum_i (\sum_\alpha e_{i\alpha}^2)^2} \right\} = \begin{cases} 34/27 & \text{for FCQ} \\ 10/3 & \text{for ICQ} \end{cases} \quad (6)$$

where $e_{i\alpha}$ is the charge of the quark with flavour *i* and colour α , is different for the different quark models while $R_{1\gamma}$ is not. Therefore it is a real challenge to measure $R_{\gamma\gamma}$ in a clean way.

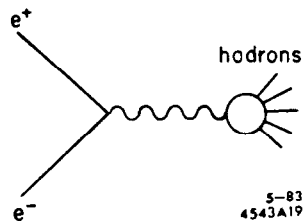


Fig. 1. e^+e^- annihilation into hadrons.

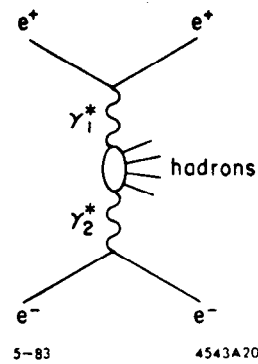


Fig. 2. Two photon production of hadrons.

- $\gamma\gamma$ scattering is a place to study the interplay between hadron-like (VDM) and pointlike coupling of the photon.
- By measuring the different underlying subprocesses like e.g. $\gamma\rho \rightarrow q\bar{q}$, $\gamma\gamma \rightarrow Mq\bar{q}$, $\rho\rho \rightarrow q\bar{q}$, ... one can test the validity of the CIM-model⁷ in $\gamma\gamma$ reactions.
- Finally, a strong challenge for the experiments is to test direct $qq \rightarrow gq$ and $q\bar{q} \rightarrow q\bar{q}$ scattering^{8,9,10} via processes as in Fig. 3 where qq -scattering is accompanied by two beam-pipe jets.

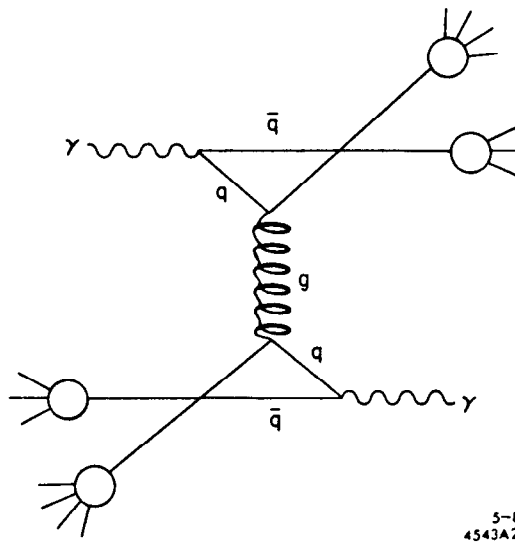


Fig. 3. Direct qq -scattering in a two photon reaction.

2. THE EXPERIMENTAL APPROACH

Let me try to describe the experimental approach to the above questions in three steps:

1. Do we have evidence for hard scattering processes in $\gamma\gamma$ reactions?
2. Can one separate the $\gamma\gamma \rightarrow q\bar{q}$ Born process from background processes?
3. To what extent can one answer the challenge questions?

Since two photon physics became accessible to high energy physics there have been six contributions to the subject of hard scattering phenomena via high p_T jets (Table I).

TABLE I

PLUTO (1980)	unpublished 1980	notag + single tag	2.6 pb^{-1}
JADE	Phys. Lett. 107B, 1981	single tag	9.7 pb^{-1}
TASSO	Phys. Lett. 107B, 1981	single tag	9.0 pb^{-1}
TASSO	preliminary 1983	notag	54 pb^{-1}
PLUTO (1982)	preliminary 1983	single tag	39 pb^{-1}
CELLO	preliminary 1983	notag	6 pb^{-1}

The published results from JADE¹² and TASSO¹³ using single tag events and the unpublished PLUTO¹¹ result have been updated by the new PLUTO detector¹⁴, dedicated to two photon physics, with much larger statistics using single tag events in two different Q^2 regions. The problem has also been attacked using notag events by TASSO and CELLO.¹⁴

Primary evidence for hard pointlike scattering in $\gamma\gamma$ -reactions should be seen in:

- (a) Jet structure of events eventually seen in single event displays,
- (b) $1/W^2$ – contribution in $\sigma_{\gamma\gamma \rightarrow had}^{tot}(W)$,
- (c) inclusive particle p_T -distributions.

The jet-like character of events seen in $\gamma\gamma$ -collisions may well be due to the Lorentz-boost of the $\gamma\gamma$ -system which makes the events appear jet-like. The presence of a $1/W^2$ -term in the parametrization of the total hadronic $\gamma\gamma$ -cross section is still under discussion¹⁵ and its existence as well as its possible origin is not yet established. Therefore we are left with the investigations referring to the last point.

As already mentioned in the Introduction, the authors of Ref.2 predicted scaling for a pointlike scattering process $a + b \rightarrow c + d$

$$E_c \frac{d\sigma}{d^3p_c} = \frac{4\pi\alpha^2}{p_T^4} f(x_T, \theta_{c.m.}) ; \quad x_T = \frac{2p_T}{\sqrt{s}} \quad (7)$$

The p_T^{-4} -term comes from a $1/s^2$ in $d\sigma/dt$ and describes the energy dependence. $f(x_T, \theta_{c.m.})$ corresponds to the angular dependence of the process. In order to “see” p_T^{-4} -behaviour of $E d\sigma/d^3p$

or $d\sigma/dp_T^2$ one must either keep x_T and $\theta_{c.m.}$ fixed or one has to make sure that the angular dependence $f(x_T, \theta_{c.m.})$ does not spoil the p_T -slope too much. An example is given in Fig. 4 for the pointlike process $e^+e^- \rightarrow \mu^+\mu^-$. The cross section is

$$\frac{d\sigma}{dp_T^2} (ee \rightarrow \mu\mu) = \frac{\alpha^2 \pi}{4s^2} \cdot \frac{1 + \cos^2 \theta}{\cos \theta} = \frac{1}{p_T^4} f(x_T, \theta_{c.m.}), \quad (8)$$

but the p_T^{-4} term is completely spoiled by the angular dependence. The cross section even exhibits a singularity at $p_T/p_T^{max} = 1$ due to the Jacobian $(\cos \theta)^{-1}$.

Usually the pointlike scattering process revealing the p_T^{-4} is only a subprocess of a more complex reaction as sketched in Fig. 5. The "hard scattering expansion"¹⁶

$$E_C \frac{d\sigma}{d^3p_C} (A + B \rightarrow C + X) = \int \int dx_a dx_b G_{a/A}(x_a, p_T^2) G_{b/B}(x_b, p_T^2) \frac{D_{C/c}}{z_c} (z_c) \times \frac{d\sigma}{dt} (a + b \rightarrow c + d) \cdot \frac{\hat{s}}{\pi} \cdot \delta(\hat{s} + \hat{t} + \hat{u}), \quad (9)$$

($\hat{s}, \hat{t}, \hat{u}$ = Mandelstam variables of the subprocess, $x_{a,b} = 2p_{a,b}/\sqrt{s}$, s = total center-of-mass energy) parameterizes this reaction in terms of structure functions $G_{x/X}$ and fragmentation functions $D_{Y/y}$ in order to convolute the subprocess and the initial and final state distributions. In the case of $\gamma\gamma \rightarrow \text{hadron} + X$ the "outer" process is $e^+e^- \rightarrow e^+e^- + h + X$. Note that for $\gamma\gamma$ reactions also the processes with more than two quarks in the final state obey the p_T^4 scaling law since the α_s in the subprocess reaction cancels against the α_s in the photon structure function as first noticed by C.H. Llewellyn Smith.⁹ Brodsky et al.⁸ and Kajantie et al.¹⁰ have performed the convolution of photon-photon flux $G_{\gamma/e}(x)$ and fragmentation function $D_{h/q}(z_h)$ with the subprocess cross section of $\gamma\gamma \rightarrow q\bar{q}$. They have shown that the p_T^{-4} -dependence is preserved for moderate x_T

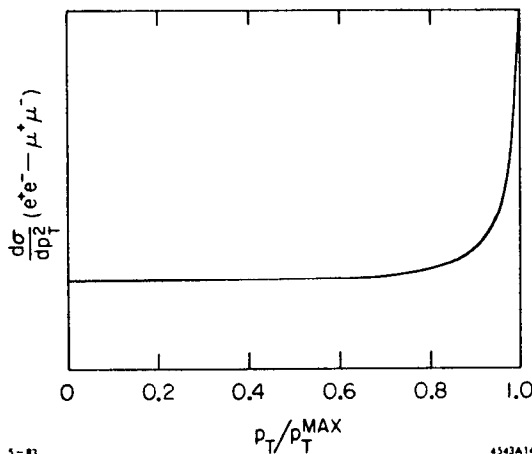


Fig. 4. $d\sigma/dp_T^2$ as function of p_T/p_T^{max} for the pointlike scattering process $e^+e^- \rightarrow \mu^+\mu^-$.

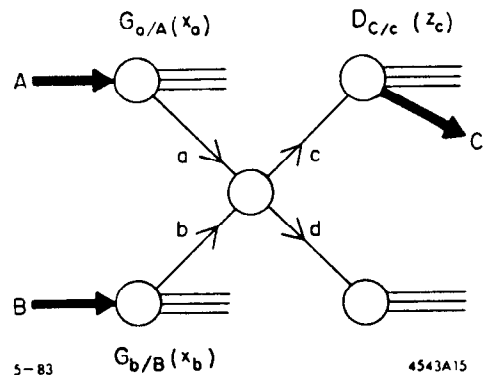


Fig. 5. The pointlike scattering process $a + b \rightarrow c + d$ embedded in the reaction $A + B \rightarrow C + D$.

$$\frac{d\sigma}{dp_T^2} (e^+e^- \rightarrow e^+e^- + h^\pm + X) \simeq \frac{1}{p_T^4} \left(\log \frac{2}{x_T} - \frac{7}{3} + \dots \right) \quad (10)$$

The angular dependence $f(x_T, \theta_{c.m.})$ only slowly varies with x_T .

This means that the experiments may integrate over p_{\perp} not keeping $x_T, \theta_{c.m.}$ fixed without affecting the p_T^{-4} -behaviour too much. Thus we would expect a flattening tail in p_T^2 -distributions of $e^+e^- \rightarrow e^+e^- + h + X$ which goes like p_T^{-n} , $n \simeq 4$. Let me remind you that for the QED-process $e^+e^- \rightarrow e^+e^- \mu^+ \mu^-$, which only has the photon structure functions in the initial state but no fragmentation in the final state, MARK J¹⁷ and PLUTO¹⁸ have measured a p_T -slope of p_T^{-n} , with $n \sim 4.2 - 4.5$, in agreement with the corresponding QED Monte Carlo calculation.

In Fig. 6 inclusive particle p_T -distributions are shown for the TASSO and PLUTO data. The TASSO data have been selected requiring ≥ 3 charged tracks in the final state. They are corrected for acceptance and compared to different slopes in p_T , normalized to each other at $p_T = 1$ GeV/c. The data at high p_T agree with p_T -slopes of p_T^{-6} and p_T^{-4} . A fit of the type $c_1 \exp(-ap_T) + c_2 p_T^{-b}$ yields $a = 7.4 \pm 0.3$ and $b = 3.9 \pm 0.6$. Although this fit result crucially depends on how the fit function is set up and how the transition between low p_T and high p_T data is parametrized, one can, I think, conclude that the data clearly break off from the exponential $\exp(-6p_T)$ behaviour, expected from a purely hadronic reaction, at $p_T \sim 1$ GeV/c and the tail at high p_T is consistent with a power law p_T^{-n} , $n \lesssim 6$. In Fig. 6(b) preliminary data from PLUTO plotted as a function of p_T^2 are directly compared to model predictions from a $\gamma\gamma \rightarrow q\bar{q}$ model (see below) and a VDM prediction which includes a limited transverse momentum phase space

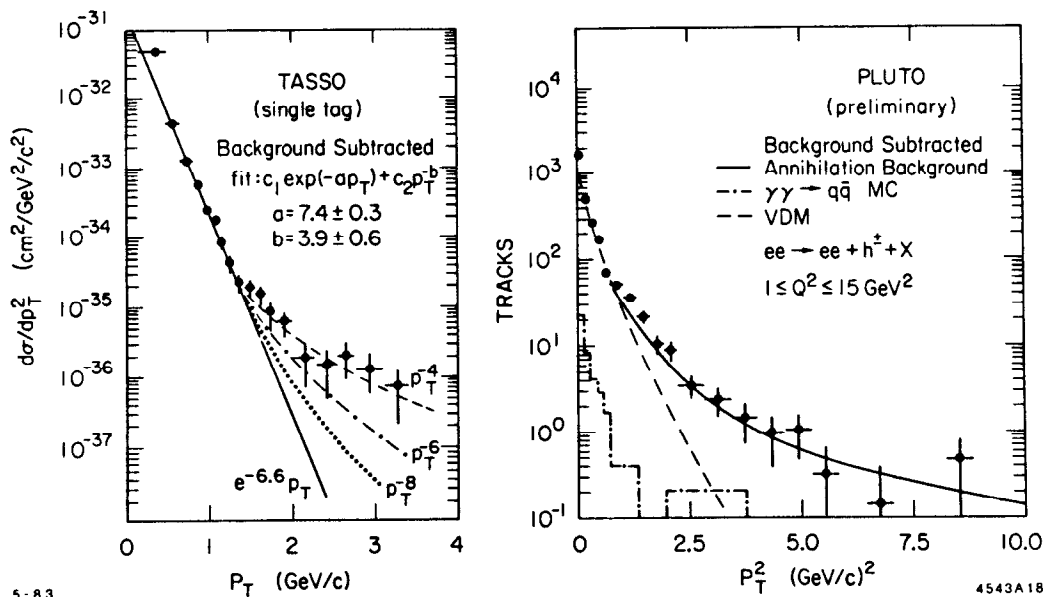


Fig. 6. (a) Inclusive particle $d\sigma/dp_T^2$ cross section observed by TASSO compared to different p_T -slopes (see text). (b) p_T^2 -distribution observed by PLUTO (LAT). The curves represent expectations from a $\gamma\gamma \rightarrow q\bar{q}$ model (solid line) and a VDM model (dashed line). The dashed-dotted line represents the 1γ background.

distribution of particles about the $\gamma\gamma$ axis. The matrix element for the latter is proportional to $\exp(-6p_T)$. These data require a tag in the PLUTO large angle tagger (LAT) resulting in a Q^2 -range from 1 to 15 GeV^2 and are selected demanding at least 4 charged tracks and a visible $\gamma\gamma$ -energy, W_{vis} , of more than 4 GeV. The above conclusion is confirmed by the PLUTO data. The high p_T tail cannot be accounted for by the VDM prediction. Since the data are not yet corrected for acceptance no attempt was made to fit the p_T -slope. The data are however consistent with p_T^{-n} , $n \lesssim 5$.¹⁹

A major concern is possible background from 1γ annihilation which may become very large at high p_T even for single tag events. In Fig. 6 this background has been computed by Monte Carlo and has been subtracted from the data. The subtraction amounts to about 15% for $p_T > 2$ GeV/c in the TASSO data. For the PLUTO data the 1γ background is shown by the histogram to be very small because of the excellent tag identification capability of the new PLUTO detector in the LAT.

For notag data the one photon background is a serious problem as shown in Fig. 7. Plotted are $\sum_i p_i/E_{beam}$ (TASSO) and W_{vis} (CELLO) respectively, with comparisons to Monte Carlo generated 1γ events. For the TASSO data some cuts for selecting high p_T events have been applied. At the high end of the distributions the data are completely explained by the annihilation process $e^+e^- \rightarrow \text{hadrons}$ when energy is lost by initial state radiation or if the final state is only partially detected. The total amount of 1γ background is $\sim 13\%$ for the CELLO data but increases to over 50% when high p_T jet events are selected. The TASSO data include $\sim 30\%$ 1γ background when a cut $\sum_i p_i/E_{beam} \leq 0.4$ is applied.

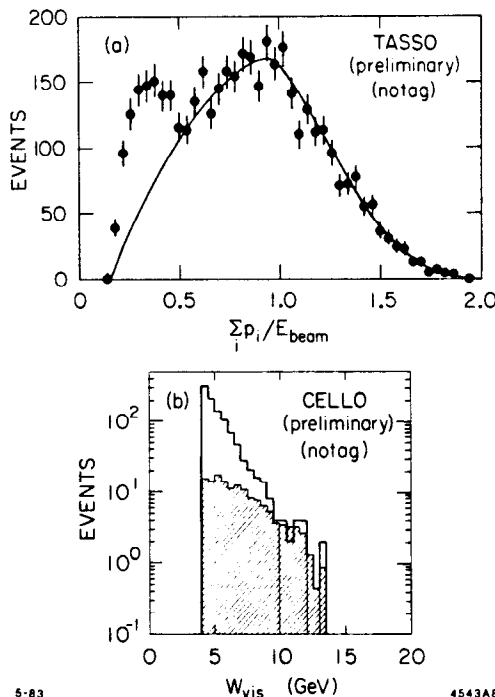


Fig. 7. Energy distributions of notag events plotted as: (a) $\sum p_i/E_{beam}$ (TASSO) and (b) W_{vis} (CELLO). The background from e^+e^- annihilation is indicated by the solid line (a) and the shaded area (b). Note that some cuts for selecting high p_T events have been made in (a).

There is no other choice for notag events than to subtract the computed amount of annihilation background in all distributions. The 1γ subtracted p_T^2 -distribution of single particles is shown in Fig. 8 for the CELLO data. Within statistics and despite the above mentioned difficulties the notag data agree with the conclusions drawn from the single tag data p_T^2 -distributions.

It is worthwhile to notice that one would expect from a hadronic behaviour of the photons ($\rho\rho \rightarrow \rho\rho$, $\gamma\rho \rightarrow \gamma\rho$)

$$E \frac{d\sigma}{d^3p} (\rho\rho \rightarrow \rho\rho) \sim p_T^{-12} \cdot f(x_T, \theta_{c.m.})$$

$$E \frac{d\sigma}{d^3p} (\gamma\rho \rightarrow \gamma\rho) \sim p_T^{-8} \cdot f(x_T, \theta_{c.m.})$$

as predicted by CIM model counting rules.²⁰ These p_T -slopes are much steeper than those seen in the data of Figs. 6 and 8.

Let me add two experimental points here. We have required the covered x_T range to be moderate in order to have the fragmentation functions and photon fluxes not affect the p_T dependence. The x_T -range covered by all experiments lies between ~ 0.1 and ~ 0.25 for high p_T tracks, i.e. moderate values. The second point is the question whether detector inefficiencies could change the conclusion. The TASSO data in Fig. 6(a) are corrected for acceptance. But apart from that the detection efficiency for high p_T tracks is almost constant above $p_T \sim 0.5$ GeV/c due to the fact that the detector acceptance is good at large angles where most of the high p_T tracks come from.

Nevertheless, before we definitely conclude that the features discussed so far give evidence for underlying hard scattering processes in $e^+e^- \rightarrow e^+e^- + h + X$ we want to directly compare to hadron-hadron data. This has been done in Fig. 9(a). The same data as in Fig. 6(a) taken at

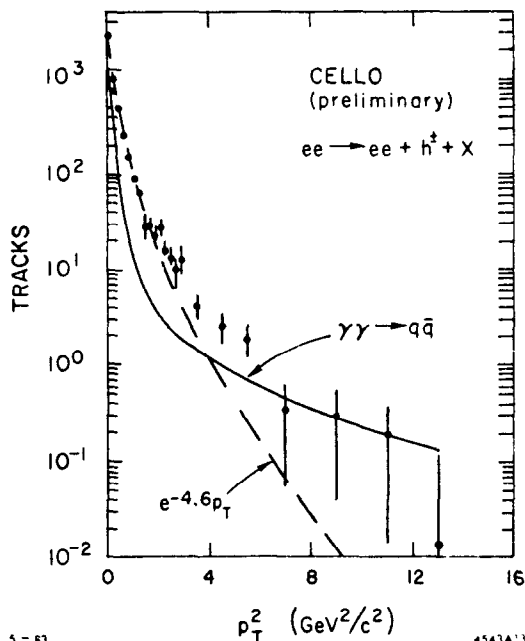


Fig. 8. p_T^2 -distribution for the CELLO notag data after subtraction of 1γ events. The curves represent the $\gamma\gamma \rightarrow q\bar{q}$ expectation (solid line) and a fit with $\exp(-4.6p_T)$ to the data.

an average e^+e^- c.m. energy of ~ 30 GeV are compared to ISR data from $pp \rightarrow \pi^\pm + X$ ²¹ at a c.m. energy of 23 GeV. The two sets of data are normalized at $p_T \sim 200$ MeV/c. The agreement at low p_T is striking. At $p_T \sim 1.5$ GeV/c however the e^+e^- data (i.e. $\gamma\gamma \rightarrow h + X$) clearly break off from the hadron-hadron slope. In Fig. 9(b) a similar comparison is made for $p\bar{p} \rightarrow h + X$ taken by the UA1 detector²² at a centre-of-mass energy of 540 GeV at the SPS collider. The data are again compared to data from ISR measurements.²¹ A similar deviation from the lower energy ISR data is observed revealing a flat high p_T tail which extends to $p_T \sim 9$ GeV/c. This effect has been attributed to underlying hard scattering subprocesses ($q\bar{q} \rightarrow q\bar{q}$) buried in the $p\bar{p}$ -reaction which become relevant at high energies and high p_T . In fact the observed p_T -slope for the UA1 data is p_T^{-n} , $n \approx 5$.²³

Therefore we conclude that for the $\gamma\gamma$ data the high p_T tail observed in $d\sigma/dp_T^2$ distributions cannot be attributed to hadron-like scattering of the photons. The alternative explanation would be to assume pointlike $\gamma\gamma \rightarrow q + X$ subprocesses to be responsible. This would give rise to events showing a jet-topology.

Before I report on jet-searches I would like to add that for a complete understanding of the inclusive particle p_T -spectra one would like to understand the following questions:

1. What is the π , K , p particle decomposition at high p_T ? How many particles are ρ 's?
2. The highest p_T bins correspond of course to low multiplicity jets due to simple kinematics. How much is just $\gamma\gamma \rightarrow \rho\rho$ scattering where the ρ 's are interpreted as two particle jets? How much is due to $\gamma\gamma \rightarrow \pi + X$ where no jets are formed?

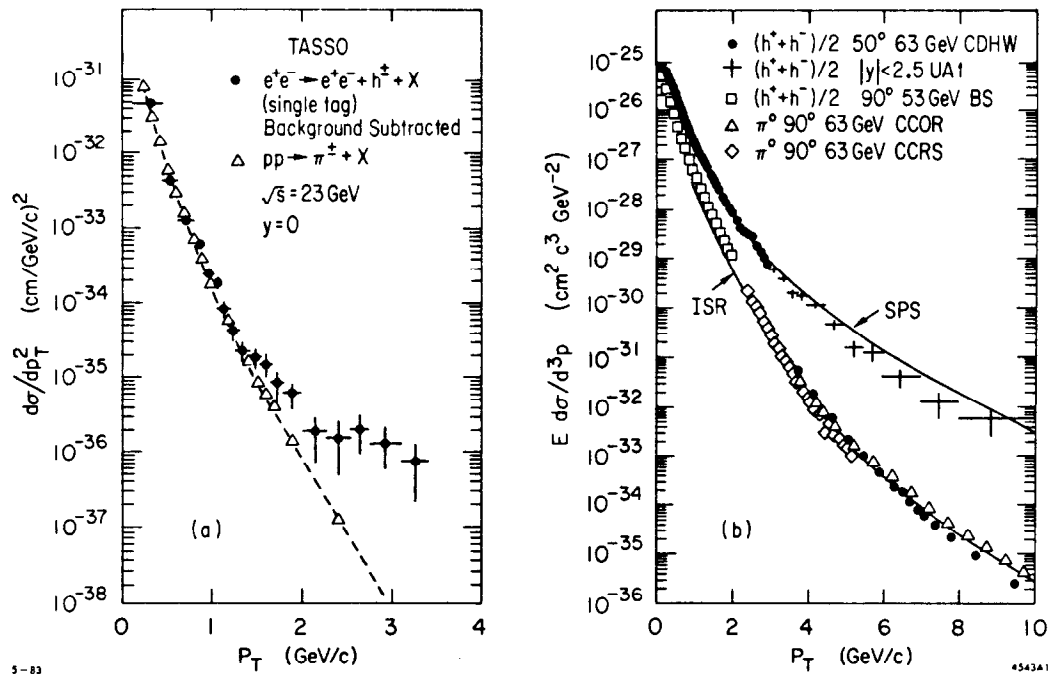


Fig. 9. (a) Comparison of the TASSO single tag data with data from Ref. 21 for $pp \rightarrow \pi^\pm + X$. (b) $E d\sigma/d^3p$ cross sections for UA1-data at $\sqrt{s} = 540$ GeV and ISR-data from Ref. 21 at $\sqrt{s} = 63$ GeV for $pp \rightarrow \pi + X$ and $p\bar{p} \rightarrow \pi + X$, respectively.

3. Although we concluded that integrating over rapidity or $\cos\theta$ was allowed for $e^+e^- \rightarrow e^+e^- + h + X$, one would nonetheless like to investigate the dependence on rapidity, i.e. measure the full differential cross section $d\sigma/dy_1 d^2p_T dy_2$.¹⁰

3. SEARCH FOR JETS

From an experimental and also theoretical point of view it is most interesting to first look for evidence for the Born term process $\gamma\gamma \rightarrow q\bar{q}$ (Fig. 10). One expects about 20-40 events per 10 pb^{-1} for tag and about 200-400 events per 10 pb^{-1} for notag events at $\sqrt{s} = 30 \text{ GeV}$ for $p_T^{\text{quark}} \geq 2 \text{ GeV}/c$ after correcting for acceptance.

The four experiments employ two different jet-finding algorithms. PLUTO and TASSO use a 'Thrust' or 'Twoplicity' method^{24,13} which always finds two jets per event. JADE and CELLO employ a cluster search algorithm^{25,12} which finds 0,1,2,3,... jet events corresponding to the number of distinct clusters found. Both methods provide jets with jet axes strongly correlated to the original quark axes as demonstrated by MC studies in Fig. 11.

There are two major concerns when searching for jets. The first concern is possible background from 1γ annihilation. This background can be reduced by requiring that the detected invariant mass of the final state must not exceed a certain maximum (usually about 40% of the e^+e^- c.m. energy). A very efficient tool is also to require a tag in the forward spectrometer which is even more powerful the better the tagging particle (e^\pm) can be identified. The new PLUTO detector has the capability to associate a tagging e^\pm with its track measured by forward drift and proportional chambers. For a LAT-tag it is also possible to measure the sign of the charge of this track from left or right bending in the forward septum magnet. This drastically reduces possible confusion by hadronic tags or γ conversion in 1γ events.

The second concern is whether one is able to extract the Born process $\gamma\gamma \rightarrow q\bar{q}$ from competing processes such as higher twist reactions⁸ and 3- and 4-jet processes.^{8,9,10} Bagger and Gunion²⁶ recently have shown that the normalization for higher twist processes, as quoted in Ref. 8, has to be corrected by a factor $\sim 1/130$. They quote for the ratio of (higher twist/minimum twist) $\sim 10\%$ at $\sqrt{s_{e^+e^-}} = 30 \text{ GeV}$ and $p_T^{\text{jet}} \geq 2 \text{ GeV}/c$. This new understanding makes life easier for the experimentalists.

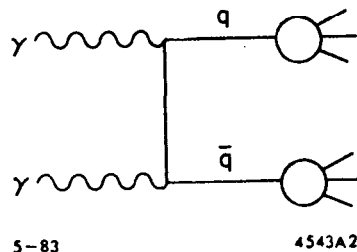


Fig. 10. The Born diagram for $\gamma\gamma \rightarrow \text{jet} + X$ reactions, $\gamma\gamma \rightarrow q\bar{q}$.

Possible identification and separation of 3- and 4-jet reactions which also scale like p_T^{-4} has been discussed by J. Stirling at this conference.²⁷ From an experimentalist's point of view, a major improvement has been made by adding forward devices to detect two photon events more completely. About 70-80% of the total $\gamma\gamma$ c.m. energy is now seen by most of the detectors for high p_T events. This is demonstrated in Fig. 12 for the PLUTO detector comparing the ratio W_{vis}/W_{true} for the old PLUTO without forward spectrometer and the new PLUTO including the forward spectrometer.

A very nice handle to suppress competing non-Born processes is to make use of large angle tags which corresponds to the photon having high Q^2 . This suppresses all kinds of $\gamma\gamma \rightarrow \text{jet} + X$ background whenever there are form factor-like effects (hadronization) involved at the high Q^2 photon vertex. Naively one would expect to reduce all higher twist and 3,4 jet backgrounds by at least about a factor of 2.

The following basic cuts were applied by the experiments when looking for jets.

- $W_{min} \leq W_{vis} \leq W_{max}$ - This cut limits the detected W_{vis} range in order to suppress 1γ background contributions (W_{max} -cut) and to provide enough energy for the quarks to develop as jets (W_{min} -cut). W_{min} is usually ~ 4 GeV, $W_{max} \sim 40\% \cdot \sqrt{s_{e^+e^-}}$.
- $n_{ch} \geq 4, n_{jet} \geq 2$ - This cut limits the jets to contain at least two particles.

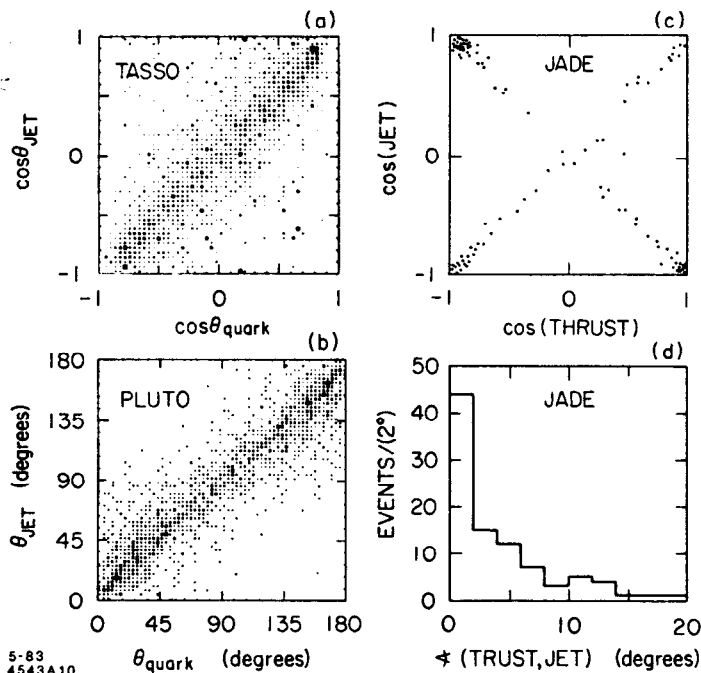


Fig. 11. MC-studies to compare jet axes and quark axes by (a) TASSO, (b) PLUTO and (c),(d) JADE employing different jet-finding methods: (a),(b) Thrust-method and (c),(d) cluster algorithm.

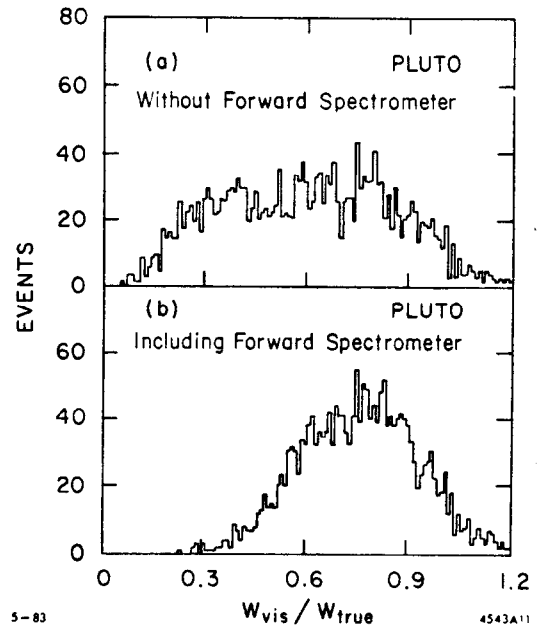


Fig. 12. W_{vis}/W_{true} for the PLUTO data without (a) and including (b) the forward spectrometer.

- Charge balance, p_T balance, p_z balance – Incomplete events especially from the 1γ process tend to be unbalanced in charge, transverse and longitudinal momentum. These cuts are therefore very useful to reduce this background.
- $p_T^{jet} > p_T^{min}$ – At least one detected jet has to have a transverse momentum greater than ~ 2 GeV/c.
- Different tagging requirements – JADE and TASSO analysed single tag events using their small angle taggers. PLUTO distinguishes between small angle tags (SAT) and large angle tags (LAT) and additionally requires that the other electron or positron is scattered under 0° , i.e. is not detected in the opposite forward spectrometer (anti-tag). Data without tag requirement were analysed by CELLO and TASSO.

Note that the first and third cut are crucial for notag data in order to reduce jet-like 1γ background.

Background from beam-gas scattering, 1γ annihilation and $\gamma\gamma \rightarrow \tau^+\tau^-$ has been computed and subtracted in all distributions. The number of events found after cuts is given in Table II.

Table II

Tagging	Experiment	Events	$MC_{1\gamma}$	$\int L dt$	
SINGLE TAG	JADE	42		$9.7 pb^{-1}$	
	TASSO	43	4.5	$9.0 pb^{-1}$	
	PLUTO	SAT	84	5	$28 pb^{-1}$
		LAT	71	2	$39 pb^{-1}$
NOTAG	TASSO	624	211	$54 pb^{-1}$	
	CELLO	128	57	$6 pb^{-1}$	

In Fig. 13 the average transverse momentum of particles with respect to the jet-axis, q_T , is plotted. It is known from e^+e^- annihilation jets at PETRA and PEP that this variable should peak at around 0.3 GeV/c. This is observed for the 2γ jet-events, too.

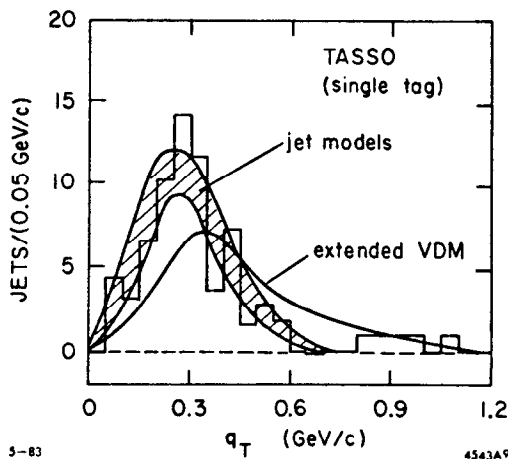


Fig. 13. Average transverse momentum q_T of particles with respect to the jet axis. Expectations from a $\gamma\gamma \rightarrow q\bar{q}$ model with different types of fragmentations (shaded area) and from a VDM model, extended such that it fits the single particle p_T -distributions, are also shown.

In order to simulate the reaction $e^+e^- \rightarrow e^+e^- + \text{jet} + \text{jet}$ all experiments employ Vermaas's QED program²⁸ to generate $e^+e^- \rightarrow e^+e^- + q\bar{q}$ according to QED and then fragment the quarks about the $q\bar{q}$ direction in the $\gamma\gamma$ c.m.-system using the standard Field-Feynman fragmentation algorithm²⁹ or a phase space model with limited p_T about the quark axis. The latter has been successfully employed when e^+e^- jets were first discovered at SPEAR.³⁰ The experiments claim that the results are fairly insensitive to the details of the fragmentation. Apart from fragmentation parameters the model has only two free parameters, the explicit quark masses and $R_{\gamma\gamma}$, the effective coupling strength. Using constituent masses for udc-quarks ($m_q = 300, 300, 500, 1500 \text{ MeV}/c^2$) one can in turn determine $R_{\gamma\gamma}$ by direct comparison between data and model predictions assuming that for high p_T events the choice of constituent masses over current masses plays a minor role.

In Fig. 14 the thrust distribution as measured by PLUTO is plotted for two different Q^2 ranges corresponding to tags in the SAT and LAT, respectively. The data are compared to the Born term prediction. The agreement is much better for the high Q^2 events indicating a better background suppression for these events as mentioned above.

The most relevant plots are shown in Figs. 15 to 17 which show the direct comparison of the data with the Born term expectation on an absolute scale (i.e. not normalized to each other). The published results from JADE and TASSO (single tag) are shown in Figs. 15(a) and 15(b). In both figures data and model approach each other at high p_T^{jet} . Note however that the statistics is poor at high p_T^{jet} . Fig. 16 shows the results for the notag approach by CELLO and TASSO. Although the same approach of data and model prediction is seen the absolute ratio between data and model is about 2 for the CELLO data whereas it is about 5 for the TASSO data. This discrepancy may be attributed to substantial difficulties in normalizing and subtracting the 1γ

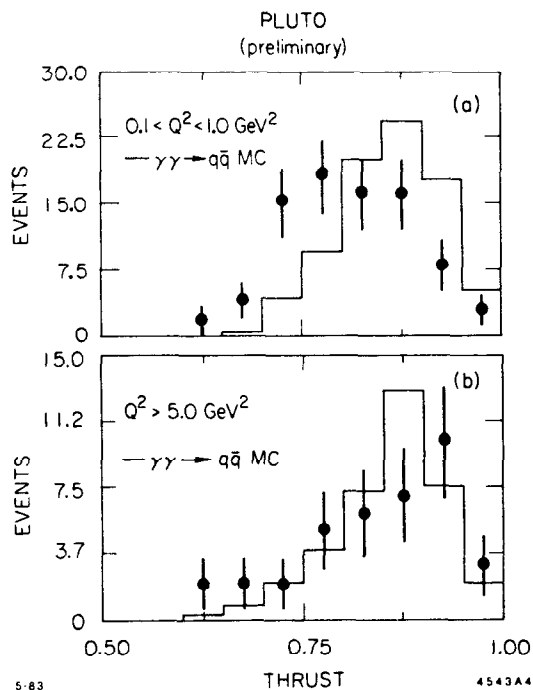


Fig. 14. Thrust distributions as measured by PLUTO compared to a MC calculation of the process $\gamma\gamma \rightarrow q\bar{q}$ for (a) SAT events ($0.1 \leq Q^2 \leq 1 \text{ GeV}^2$) and (b) LAT events ($Q^2 > 5 \text{ GeV}^2$).

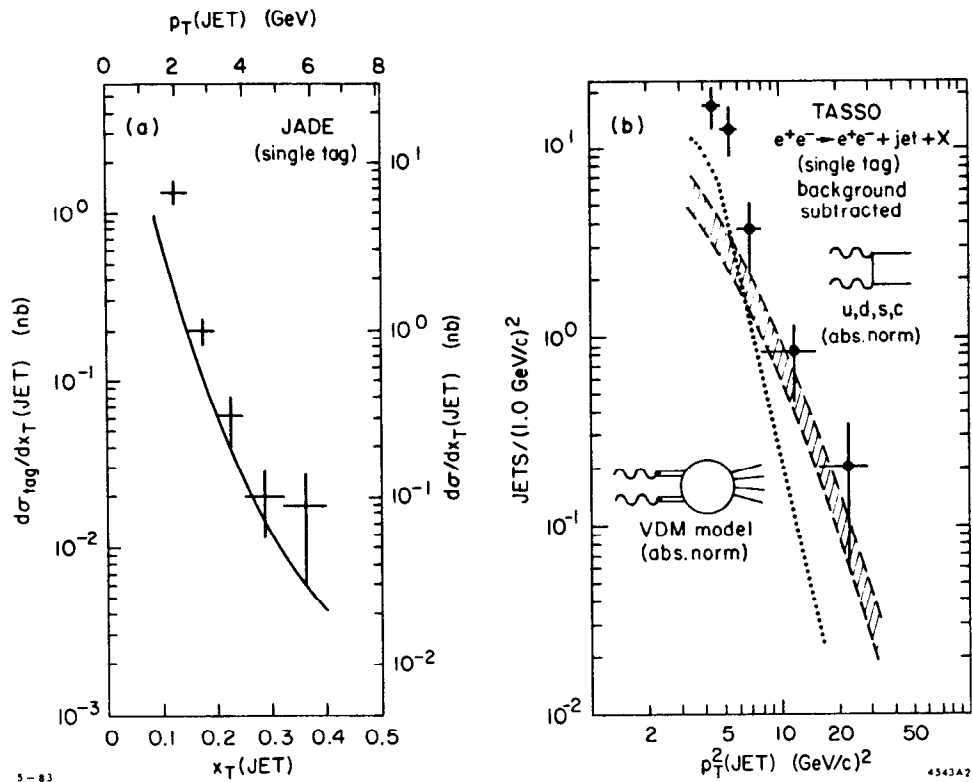


Fig. 15. Jet- p_T cross sections for the JADE (a) and TASSO (b) single tag data, $x_T = 2p_T/\sqrt{s}$. (a) The solid line represents the $\gamma\gamma \rightarrow q\bar{q}$ MC calculation. (b) The shaded area represents a $\gamma\gamma \rightarrow q\bar{q}$ calculation using for the fragmentation the standard Field-Feynman model and a limited- p_T phase space model with different parameter sets. The dotted line represents the VDM model prediction.

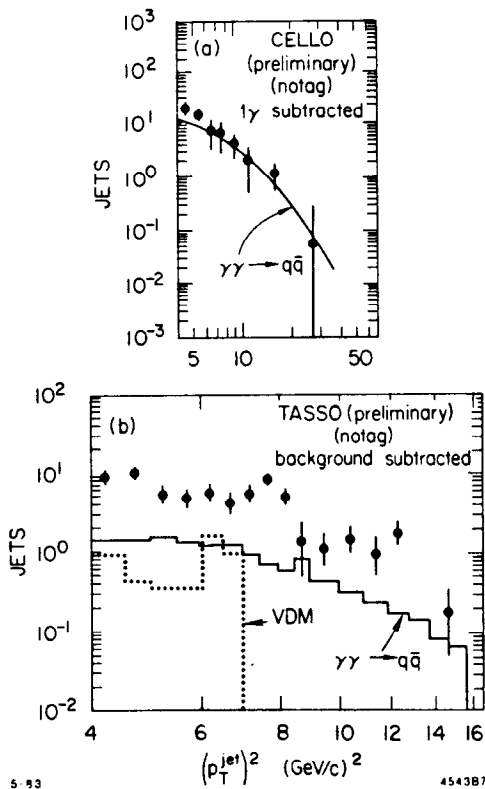


Fig. 16. Jet- p_T^2 distributions for notag events from (a) CELLO and (b) TASSO compared to models.

background. It seems unlikely that the different cuts and event selection methods can account for this effect. Very important progress has been made by PLUTO in Fig. 17 showing the same distributions for events with high (LAT) and low Q^2 (SAT) photons. Again, as already seen for the thrust distributions, the agreement at high p_T between data and the Born term reaction is much better for the high Q^2 events. The data are not yet corrected for acceptance. The indicated amount of 1γ background demonstrates how clean these measurements are.

We now define

$$\tilde{R}_{\gamma\gamma} = \frac{d\sigma/dt(\gamma\gamma \rightarrow jet + X)}{d\sigma/dt(\gamma\gamma \rightarrow \mu\mu)}$$

which is always greater than or equal to

$$R_{\gamma\gamma} = \frac{d\sigma/dt(\gamma\gamma \rightarrow q\bar{q})}{d\sigma/dt(\gamma\gamma \rightarrow \mu\mu)}$$

since other (non-Born term) hard scattering $\gamma\gamma$ reactions are likely to contribute. For increasing p_T^{jet} ($x_T \rightarrow 1$) we expect $\tilde{R}_{\gamma\gamma}$ to approach $R_{\gamma\gamma}$ as the competing processes die faster with p_T at fixed s .

In Fig. 18 $\tilde{R}_{\gamma\gamma}$ is plotted for the TASSO single tag data as a function of the p_T -cut. Also shown are the predictions from the naive ICQ model (10/3) and the FCQ model (34/27). Figures 19(a) and 19(b) show $\tilde{R}_{\gamma\gamma}$ for the PLUTO low and high Q^2 data respectively as a function of p_T (not p_T^{min} !). In all three figures the data approach the FCQ model expectation at high p_T where $\tilde{R}_{\gamma\gamma}$ is expected to be closer to $R_{\gamma\gamma}$. The naive ICQ model seems to be ruled out although the errors are large. It is remarkable that for the high Q^2 events $\tilde{R}_{\gamma\gamma}$ is almost flat and is always close to the FCQ expectation, again reflecting the fact that competing subprocesses are Q^2 -suppressed.

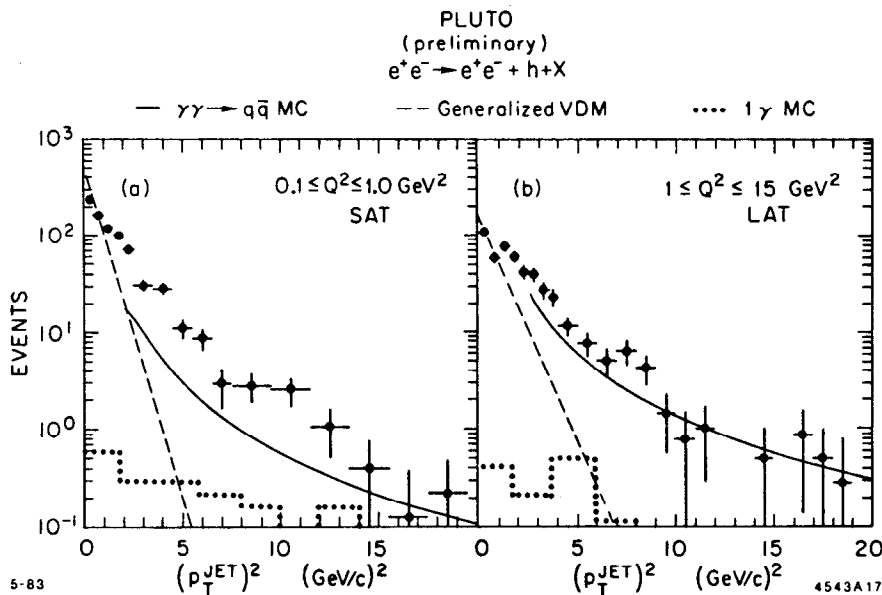


Fig. 17. Jet- p_T distributions for different Q^2 ranges of the tagged photon made by PLUTO; (a) $0.1 \leq Q^2 \leq 1 \text{ GeV}^2$ and (b) $1 \leq Q^2 \leq 15 \text{ GeV}^2$. The solid line represents the $\gamma\gamma \rightarrow q\bar{q}$ calculation. The histogram represents the amount of 1γ background.

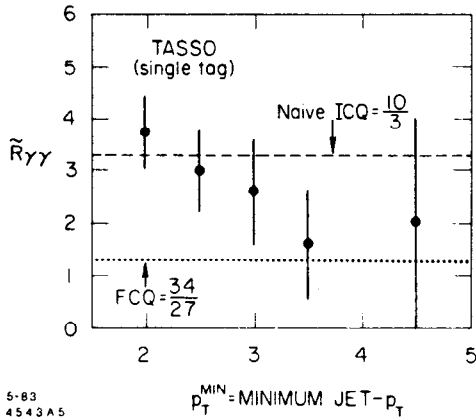


Fig. 18. $\tilde{R}_{\gamma\gamma} = [d\sigma/dt(\gamma\gamma \rightarrow jet + X)] / [d\sigma/dt(\gamma\gamma \rightarrow \mu\mu)]$ plotted as a function of the p_T^{jet} -threshold p_T^{min} (TASSO). The expectations from FCQ and ICQ models are shown as horizontal lines.

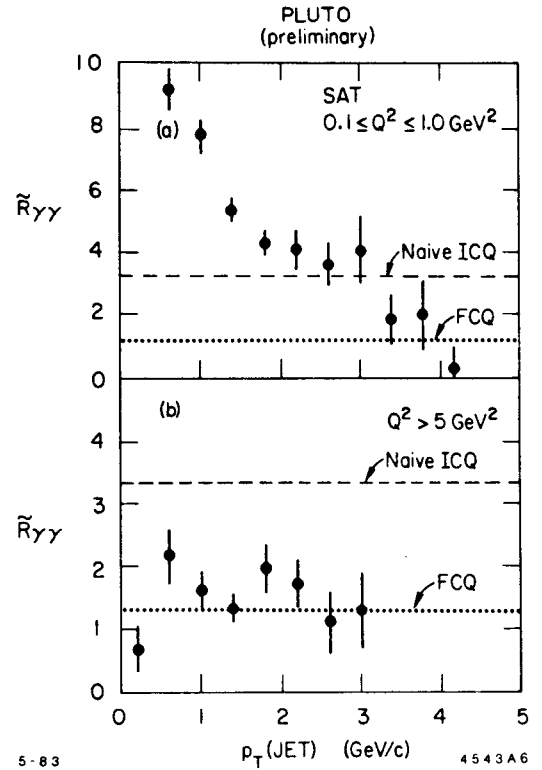


Fig. 19. $\tilde{R}_{\gamma\gamma} = [d\sigma/dt(\gamma\gamma \rightarrow jet + X)] / [d\sigma/dt(\gamma\gamma \rightarrow \mu\mu)]$ for the PLUTO data; (a) $0.1 \leq Q^2 \leq 1 \text{ GeV}^2$ and (b) $Q^2 > 5 \text{ GeV}^2$. The horizontal lines represent expectations from FCQ and ICQ models.

4. ANSWERS AND CONCLUSIONS

In this conclusion, I want to assess to what extent we have been able to approach the challenging questions phrased in the beginning.

1. I think we can say that hard scattering processes in $\gamma\gamma$ -reactions probably do exist. The evidence is most convincing from inclusive particle $d\sigma/dp_T^2$ distributions, particularly when comparing directly to hadron-hadron data, and from jet searches. The observation of high p_T particles cannot be explained by VDM model calculations nor by extrapolating hadron-like behaviour of the photon from hadron-hadron reactions. Substantial progress has been made to establish the Born term process $\gamma\gamma \rightarrow q\bar{q}$ by suppressing competing processes through a selection of high Q^2 events.
2. At first glance the measured values of $\tilde{R}_{\gamma\gamma}$, particularly at high p_T^{jet} seem to rule out the ICQ model values of quark charges. But this is only true for non-gauge ICQ models of the naive Han-Nambu-type. For so-called gauge-ICQ models³¹ this statement no longer

holds.³² We have seen that the $\{8\}_C$ part of the photon is responsible for a larger value of $R_{\gamma\gamma}$ in ICQ models. But this allows direct photon-gluon coupling to occur in $\gamma\gamma \rightarrow q\bar{q}$ scattering (Fig. 20) which modifies the effective quark charge seen by the photon by introducing a propagator-type suppression

$$Q_{eff}(q^2) = Q_{\{1\}_C} + \frac{m_g^2}{m_g^2 - q^2} Q_{\{8\}_C} \quad (11)$$

where $Q_{\{1\}_C}$ = colour singlet charge, $Q_{\{8\}_C}$ = colour octet charge, q^2 = photon 4-momentum squared and m_g = gluon mass. This means that for $q^2 = 0$, i.e. notag events, Q_{eff} is equal to the sum of $Q_{\{1\}_C}$ and $Q_{\{8\}_C}$. For $q^2 \neq 0$, i.e. single or double tag events, the colour-octet charge is suppressed. In the limit of $q^2 \rightarrow \infty$ Q_{eff} becomes $Q_{\{1\}_C}$ and therefore $R_{\gamma\gamma}^{ICQ}$ will approach $R_{\gamma\gamma}^{FCQ}$ when q^2 increases. The authors of Ref. 33 estimated the gluon mass m_g using the JADE and TASSO single tag data.^{12,13} They concluded from these data that

$$m_g \lesssim 200 - 300 \text{ MeV}/c^2 .$$

Untagged data ($Q^2 = 0$) will be required to decide whether the ICQ models are ruled out or not.

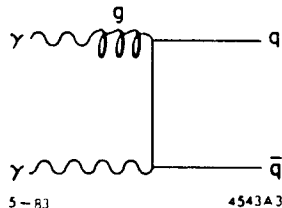


Fig. 20. Feynman diagram for direct photon-gluon coupling in $\gamma\gamma \rightarrow q\bar{q}$ reactions. This diagram requires the photon to carry colour-charge.

3. No real test has been performed so far on the magnitude of the quark propagator in Fig. 10. All differences between data and model predictions were attributed to $R_{\gamma\gamma}$. On the other hand, no dramatic deviations from the standard QED propagator have been observed which would imply that QED is not valid for photon-quark interactions. Most of the experiments are insensitive to whether current or constituent masses are the right quark masses in the propagator. At high p_T the quark mass is only a small correction. Experiments with forward angle coverage (PLUTO and PEP9 at PEP) should be able to attack this question looking for small angle jets.
4. The predicted scale invariance of pointlike scattering processes is strongly indicated in inclusive particle $d\sigma/dp_T^2$ distributes at high p_T . The direct comparison to pp and $p\bar{p}$ data shows very nicely that scaling is achieved at much lower energies than in hadron-hadron reactions. The errors are still too big for a firm conclusion on this issue for the jet-trigger $d\sigma/dp_T^2(\text{jet})$ cross sections.

5. Data at different Q^2 are very important and helpful to disentangle the different contributions of the subprocesses to the $\gamma\gamma \rightarrow \text{jet} + X$ reaction. Encouraging preliminary results from PLUTO have been shown in this talk. I think it is the theorists' turn now to tell us what impact the PLUTO data have on the understanding of how the different underlying subprocesses contribute.
6. A positive identification of CIM-subprocesses is still lacking. There is also only little hope that this will be achieved very soon because our understanding of the relative importance of these processes has been modified quite a lot. This is, on the other hand, very fortunate if one is concerned about processes confusing a clean measurement of the Born term process.
7. A big challenge for the dedicated two-photon experiments PLUTO and PEP9 is to look for direct γq - and $q \bar{q}$ -scattering subprocesses like the one in Fig. 3. A major warning has always been that it is extremely difficult to identify beam-pipe jets. But a very nice indirect approach would be to perform an "anti-beam-pipe-jet" cut, i.e. requiring that the forward spectrometers did not detect hadrons. Just comparing the $\gamma\gamma \rightarrow \text{jet} + X$ cross sections with and without this cut would already provide a first result for the relative importance of these 3- and 4-jet processes.

Let me finish with a word of caution. As first noticed by Berends et al.³⁴ and recently worked out in more detail by Kang³⁵ using the Serman-Weinberg definition³⁶ of jets, the QCD corrections to the lowest order process $\gamma\gamma \rightarrow q \bar{q}$ are expected to be large in the p_T and \sqrt{s} range of the present experimental data. This would not modify the experimental observations presented here but would change the interpretation of the data in terms of $R_{\gamma\gamma}$.

ACKNOWLEDGEMENTS

I am very grateful for private communications and discussions with S. Cartwright and A. Tylka (PLUTO), D. Cords (JADE), H. Lierl (CELLO) and E. Duchovni (TASSO) on the special aspects of the different experimental data and for providing preliminary and unpublished results for this report. I would like to thank S. Brodsky and A. Janah for valuable discussions. I very much appreciate the support I have received from my colleagues at DESY, BONN and SLAC while preparing the talk and finishing the manuscript. Finally I want to thank Prof. C. Berger and his staff for the hospitality extended to me at this interesting conference.

REFERENCES

1. For instance, J. F. Gunion, talk given at the 3rd International Colloquium on $\gamma\gamma$ Collisions, Amiens, 1980, Lecture notes in Physics No. 134 (1980); S. Brodsky, talk presented at the 4th International Colloquium on Photon-Photon Interactions, Paris, 1981, World Scientific, Singapore (1981).
2. S. M. Berman, J. D. Bjorken and J. B. Kogut, Phys. Rev. D 4, 3388 (1971).
3. See e.g., F. E. Close, An Introduction to Quarks and Photons, Academic Press, London, 1979.
4. Y. Ne'eman, Nucl. Phys. 26, 222 (1961); M. Gell-Mann, Phys. Rev. 125, 1067 (1962); O. W. Greenberg, D. Zwanziger, Phys. Rev. 150, 1177 (1966).
5. M. Y. Han and Y. Nambu, Phys. Rev. 139B, 1006 (1965).
6. M. Chanowitz, Proceedings of the 12th Rencontre de Moriond, 1977, ed. Tran Thanh Van; S. J. Brodsky, talk given at the J. Weis Memorial, Seattle, 1978, SLAC-PUB 2240; P. Landshoff, Proc. Lep Summer Study, Les Houches, 1978, CERN 79-01, P. 555; H. K. Lee, ICTP Preprint, IC/78/95, Trieste, Italy.
7. R. Blankenbecler, S. Brodsky and J. F. Gunion, Phys. Rev. D 18, 900 (1978).
8. S. Brodsky, T. A. DeGrand, J. F. Gunion and J. H. Weis, Phys. Rev. D 19, 1418 (1979); and Phys. Rev. Lett. 41, 672 (1978).
9. C. H. Llewellyn Smith, Phys. Lett. 79B, 83 (1978).
10. K. Kajantie, Proceedings of the 4th International Colloquium on $\gamma\gamma$ Collisions, Paris, 1981, World Scientific, Singapore (1981); K. Kajantie and R. Raitio, Nucl. Phys. B159, 528 (1979).
11. W. Wagner, Proceedings of the International Conference on High Energy Physics, Madison, 1980, p. 576.
12. W. Bartel et al., Phys. Lett. 107B, 163 (1981).
13. R. Brandelik et al., Phys. Lett. 107B, 290 (1981).
14. See also: H. Spitzer, summary of discussion sessions, this conference.
15. H. Kolanoski, talk given at this conference.
16. W. Caswell, R. Horgen and S. Brodsky, Phys. Rev D 18, 2415 (1978).
17. MARK J Collaboration, B. Aderva et al., Phys. Rev. Lett. 48, 721 (1982).
18. M. Pohl, talk given at this conference.
19. S. Cartwright, PLUTO Collaboration, private communication.
20. S. Brodsky and G. Farrar, Phys. Rev. D 11, 1309 (1975).
21. B. Alper et al., Nucl. Phys. B100, 237 (1975).

22. G. Arnison et al., Phys. Lett. 118B, 167 (1982).
23. M. Yvert, talk given at the Intern. Symp. on High Energy Physics, Vanderbilt (1982).
24. S. Brandt et al., Phys. Lett. 12, 57 (1964); E. Fahri et al., Phys. Rev. Lett. 39, 1587 (1977).
25. K. Lanius, preprint DESY 80/36 (1980); H. J. Daum, H. Meyer and J. Buerger, Z. Phys. C8, 167 (1981).
26. J. A. Bagger and J. F. Gunion, University of California, Davis, Preprint UCD-83/1.
27. J. Stirling, talk given at this conference.
28. J. A. M. Vermaseren, Proceedings of the International Colloquium on $\gamma\gamma$ Collisions, Amiens, 1980, Lecture notes in Physics No. 134, Springer, 1980.
29. R. D. Field and R. P. Feynman, Nucl. Phys. B136, 1 (1978).
30. G. Hansen et al., Phys. Rev. Lett. 35, 1609 (1975).
31. J. C. Pati, A. Salam, Phys. Rev. D 8, 1240 (1973), Phys. Rev. D 10, 275 (1974); J. C. Pati and A. Salam, Phys. Rev. Lett. 36, 11 (1976); G. Rajasekaran and P. Roy, Phys. Rev. Lett. 36, 355 (1976).
32. A. Janah and M. Özer, University of Maryland, PUB-81-221; A. Janah, Doctoral dissertation, University of Maryland (1982).
33. T. Jayaraman, G. Rajasekaran and S. D. Rindani, Phys. Lett. 119B, 215 (1982); K. H. Cho, S. H. Han and J. K. Kim, Phys. Rev. D 27, 684 (1983).
34. F. A. Berends et al., DESY 80/89 (1980); F. A. Berends et al., Phys. Lett. 92B, 186 (1980).
35. I. Kang, Preprint Oxford TP 50/82; see also J. Stirling, talk given at this conference.
36. G. Sterman and S. Weinberg, Phys. Rev. Lett. 39, 1436 (1977).